

Laser ion source development for the Columbia University microbeam

A. W. Bigelow,^{a)} G. Randers-Pehrson, and D. J. Brenner
Center for Radiological Research, Columbia University, New York, New York 10032

(Presented on 4 September 2001)

A design is given of a laser ion source for the 4.2 MV Van de Graaff accelerator at the Columbia University Radiological Research Accelerator Facility (RARAF). The source has been designed with application in mind for the RARAF single-particle single-cell microbeam, though it will also be used for broad-beam irradiations. The operating principle, laser ablation, can produce heavy ions with high charge states so that their energies will be high enough to provide sufficient range—at least 20 μm —for irradiating cells on a thin surface at atmospheric pressure. The laser ion source being implemented at RARAF is based on the laser operated ion source used by Hughes at the University of Arkansas and consists of three main components: laser generator, source vacuum chamber, and spherical electrostatic analyzer. © 2002 American Institute of Physics.

[DOI: 10.1063/1.1427348]

I. INTRODUCTION

Columbia University's Radiological Research Accelerator Facility (RARAF) conducts fundamental investigations into the radiobiological effects on mammalian cells through controlled single-particle single-cell microbeam irradiation. The ion source that is currently used on our 4.2 MV Van de Graaff particle accelerator, a duoplasmatron, ionizes atoms from the gaseous phase and is suitable for alpha particle irradiation experiments.¹ However, to extend the linear energy transfer (LET) range of our experiments, highly charged heavy ions are necessary. Expectations are that a laser ion source will enable a range of ions from hydrogen to around iron with an approximate LET range of 10 to 4500 keV/m.

Laser ion sources have been developed and are used at several particle accelerator laboratories.² Many of these ion sources share a common mechanism of plasma generation through laser ablation of a solid target. Particles are evaporated from a target using a focused high-energy pulsed laser. Plasma electrons are heated by the laser radiation to temperatures up to several hundreds of eV. High charge states are produced by electron-ion collisions. The temperature of the plasma and the consequent final ion charge-state distribution strongly depend on the laser power density on the target.³ A useful trait common among contemporary laser ion sources is the directional nature of the plasma plume; ion extraction is preferred along the direction normal to the target.

II. LASER ION SOURCE PROTOTYPE

The laser ion source development at RARAF is based on a prototype built from components of the laser operated ion source (LOIS) used by Hughes at the University of Arkansas.⁴ The prototype construction involved reviving and optimizing a 1970's Holobeam 5050Q Nd:YAG laser and assembling a vacuum system component containing the ion source target material, a cylindrical electrostatic analyzer

(ESA), two Einzel lenses (ion optical focusing elements), and a microchannel plate (MCP) particle detector. In order to attain proof of principle while maintaining result comparison capabilities, the prototype construction followed specifications for the most recent version of LOIS.⁵ A schematic of the laser ion source prototype is shown in Fig. 1.

The laser beam enters the vacuum system through a window and passes through a lens (focal length $f = 12.2$ cm) and impinges on the target at an 8.5° angle of incidence. In the Q -switched mode and with two stages of amplification, specifications for the Holobeam laser indicated maximum energy $E = 850$ mJ, pulse duration $t = 15$ ns, and wavelength $\lambda = 1.064$ μm .⁶ Laser spot scores on blackened paper provided a beam diameter measurement $D = 0.38$ cm. From optics theory, one can calculate the focused beam spot diameter $d = 1.22 \lambda f / D = 42$ μm . This leads to a power density idealization of 4.1×10^{12} W/cm².

A motor continually turns a cylindrical target at 6 min per revolution so that each laser pulse strikes a fresh surface. The diameter of the target is 6.15 cm and has a 19.3 cm circumference. The diameter of an ablation crater in aluminum is 0.25 mm. Hence, there is room for 770 individual craters about the target circumference. For one target rotation, the system frequency is $770 / (6 \text{ min}) = 2.1$ Hz. The laser repetition rate is set to this frequency. After one target rotation, the target is translated 0.25 mm.

Plasma expansion occurs over a drift distance of 70 cm; this distance fits within the range of typical drift distances for laser ion sources according to Sharkov.³ Furthermore, the drift distance leads to an increased temporal ion pulse width and to a reduction in subsequent plasma effects, such as plasma shielding and arcing, when the ions enter an electrostatic field region.^{3,7} Afterwards, the plasma plume enters an electrostatic analyzer consisting of a pair of cylindrical plates that bend the ions through 180° . The analyzer, tuned for energy per charge, will considerably reduce the beam load on the accelerator vacuum system. For infinitely tall coaxial cylinders, electrostatic theory states that the ions are analyzed by kinetic energy $E = kV_A z$, where k is the analyzer constant

^{a)}Electronic mail: ab1260@columbia.edu

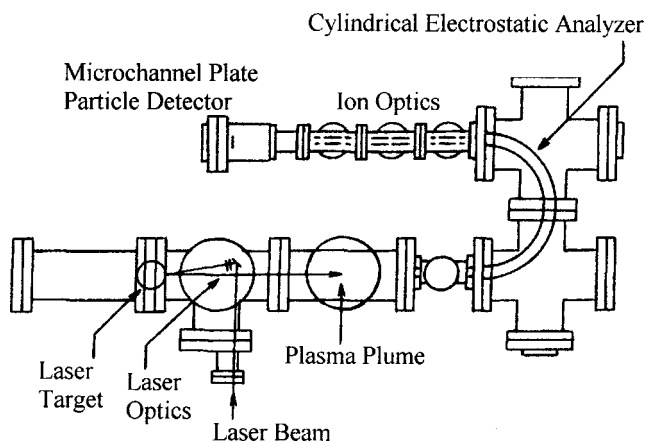


FIG. 1. Schematic of laser ion source prototype used to demonstrate proof of principle.

$\sim 5.62 \text{ eV/V}$, V_A is the voltage across the analyzer, and z is the ion charge state.⁸ Next along the ion optical path, two Einzel lenses are available to guide ion trajectories towards the MCP particle detector. The MCP axial position matches the eventual position of the particle accelerator entrance aperture. Attached to the MCP are a series of signal detection electronics and a computer that runs a digitized waveform acquisition program in LabVIEW.⁹

III. PLASMA CHARACTERISTICS

With an operational laser ion source, research was steered towards the intricate details of laser-induced plasmas. System calibration involved time-of-flight (TOF) spectra of aluminum ions. A sample TOF spectrum for aluminum with the ESA set for 400 eV/z is shown in Fig. 2. This spectrum incorporated an average of 128 system cycles. The stray-light background peak initiated by plasma light reflections offered a convenient start time pulse. From plasma formation to the particle detector, the total flight distance for these ions was 1.65 m. In comparison with kinematic theory, TOF data for a variety of ion energies had a consistent offset in time. The experimental ions required more time, implying that a reduced electric field in the ESA diminished ion analysis in terms of energy per charge. Possible explanations for this

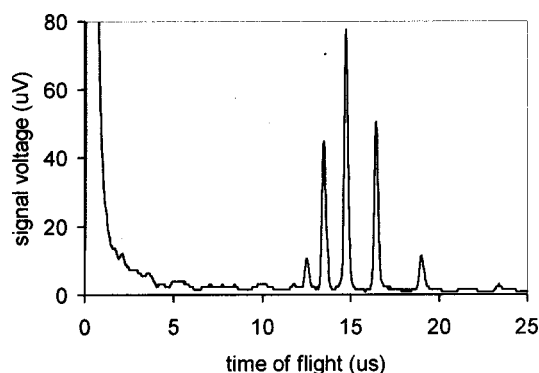


FIG. 2. TOF spectrum for 400 eV/z aluminum from the laser ion source prototype. Arrival times for consecutive charge state peaks for Al^{+8} to Al^{+2} were 11.8, 12.52, 13.48, 14.72, 16.44, 19.04, and $23.4 \mu\text{s}$.

offset are from plasma shielding effects, from ESA voltage settings based on theoretical infinitely high coaxial cylinders, or from a physical shift in the ESA cylindrical electrode locations.

Ion signal production does depend on target surface condition and laser power density. There was a significant reduction in high charge-state yield when plasma was generated from a target surface that had been ablated. So, for high charge-state production, it is important to coordinate target advancement with laser ablation. As laser power density increased, the average charge state increased. At lower laser power densities, for instance, there is a peak for Al^{+1} ; it dissipates in favor of higher charge states as laser power density increases.

Critical plasma details for the laser ion source design include the energy and angle distribution of the most highly charged ions. It is necessary to know where the greatest abundance of these ions resides in order to guide them to the entrance of the particle accelerator. Hughes reported a radial distribution in an extracted laser-plasma ion beam where the fastest ions, also those with the highest charge states, reside on the outside of the beam;⁴ space-charge repulsion effects were used to explain the trend. Data generated from the laser ion source prototype, however, suggest that the greatest abundance of the highly charged ions was slower (less energy) and was concentrated along an emission direction normal (perpendicular) to the target material. This was achieved using magnetic coil deflectors to sample the angular emission of the plasma plume.

IV. COMPUTER SIMULATION

Ion trajectories through the laser ion source prototype were simulated with an ion optics computer program, SIMION.¹⁰ The simulation consisted of virtual ion optical components arranged on an ion optics workbench. Ions flown through the system provided ion trajectory data useful in characterizing the source emittance. For a confidence check, TOF values from these data compared well with kinematic theory.

Ideally, the laser ion source emittance should match well with the 1/8-in.-diam entrance aperture to the particle accelerator; this calls for an ion optical system with point-to-point focusing. Use of a cylindrical ESA followed by two Einzel lenses prohibited this condition. Voltage configurations on these lenses could focus the ions in either the vertical or the horizontal plane, but not simultaneously. An example of emittance patterns for an acceptable vertical focus of 400 eV/z aluminum ions originating from a 0.25 mm laser ablation crater is shown by the phase space plots in Fig. 3. Voltages used to generate this emittance were: 69.35 V across the analyzer, -200 V on the first Einzel lens, and 100 V on the second Einzel lens. A random generator was used for divergence within a 1° cone angle. The focusing conditions portrayed in Fig. 3 were typical for the laser ion source prototype; simultaneous focusing in both horizontal and vertical planes was not possible.

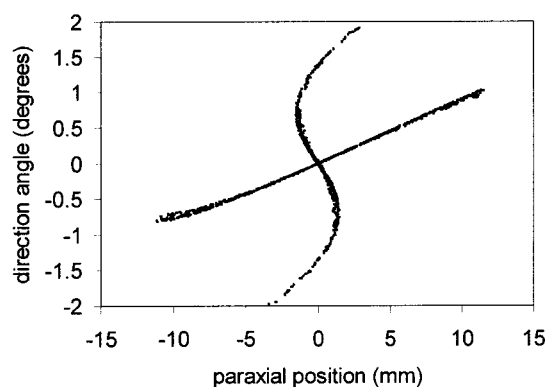


FIG. 3. Emittance simulation from the laser ion source prototype. Acceptable vertical focus is represented by the upright s-shaped pattern. The line pattern describes a broad unfocused horizontal component.

V. LASER ION SOURCE DESIGN

The laser ion source development for the Columbia University microbeam incorporates a spherical ESA. This specific type of analyzer has double focusing capabilities with point-to-point focusing in both the horizontal and vertical planes. Spherical ESA theory and fringing field effects are well documented in Wollnick's treatment of electrostatic prisms.¹¹ Guided by spatial limitations in the particle accelerator and by a desired plasma expansion drift distance of 70 cm the ESA dimensions were narrowed to a 24° bend with a 2.7 in. radius. This geometrical solution was found by applying Barber's rule; the object point, the center of curvature, and the image point lie on a straight line.¹² A diagram of the laser ion source inside its spatial confines is shown in Fig. 4.

The laser ion source to be implemented on the Columbia University microbeam will include a contemporary laser. Factors important to the laser purchase decision are power

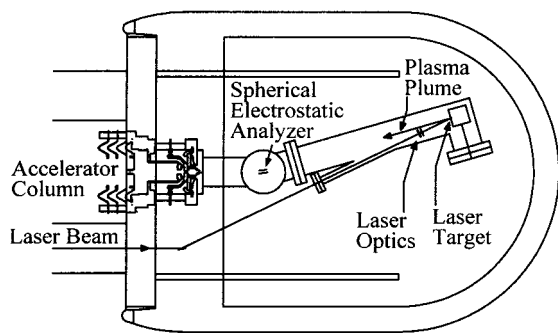


FIG. 4. Top view diagram of the proposed laser ion source inside the particle accelerator terminal dome.

and repetition rate requirements. With today's laser technology, pulsed lasers still provide greatest power. As for repetition rate, the desired experimental error of controlled particle irradiation restricts one particle irradiation per 100 laser shots. Repetition rates greater than 1000 Hz would keep the laser pulsing frequency from being a rate limiting step. Costly commercial Ti:sapphire lasers can meet both these requirements. Budget friendly commercial Nd:YAG lasers provide the power requirement, but, they are limited to 100 Hz repetition rates. Combinations of multiple Nd:YAG lasers, synchronized with temporal offsets could reduce a repetition rate handicap.

Outlining the laser ion source implementation, a 100 Hz Nd:YAG laser will be mounted in front of the Van de Graaff accelerator, parallel to and alongside the charged particle beam line. The light beam from the laser will enter the base of the accelerator through an existing window. Inside the accelerator, the light will pass through one of the insulating support tubes to the terminal where it will be directed toward the window of the ion source vacuum chamber. With harmonic generation, a variety of laser wavelengths (1064, 532, and 355 nm) leads to flexibility concerning potential attenuation in the accelerator's insulating gas and wavelength-dependent ablation yields.¹³ The insulating gas is presently a mixture of N_2-CO_2 at 10 atm and it is possible that SF_6 will be used in the future. Ultimately, the vacuum chamber component to the laser ion source will be a modular unit, interchangeable with the duoplasmatron gas ion source.

ACKNOWLEDGMENTS

This work was supported by NIH Grant Nos. RR-11623 and CA-49062.

- ¹G. Randers-Pehrson, C. R. Geard, G. Johnson, C. D. Elliston, and D. J. Brenner, *Radiat. Res.* **156**, 210 (2001).
- ²P. Fournier *et al.*, *Rev. Sci. Instrum.* **71**, 1405 (2000).
- ³B. Sharkov, in *Handbook of Ion Sources*, edited by B. Wolf (Chemical Rubber, Boca Raton, 1995), p. 149.
- ⁴R. H. Hughes, R. J. Anderson, C. K. Manka, M. R. Carruth, L. G. Gray, and J. P. Rosenfeld, *J. Appl. Phys.* **51**, 4088 (1980).
- ⁵R. D. Miller, G. Wattuhewa, R. H. Hughes, D. O. Pederson, and X. M. Ye, *Phys. Rev. B* **45**, 12 019 (1992).
- ⁶R. D. Miller, Ph.D. thesis, The University of Arkansas, 1990.
- ⁷I. G. Brown, in *The Physics and Technology of Ion Sources* (Wiley, New York, 1989), pp. 11 and 12.
- ⁸X. M. Ye, Ph.D. thesis, The University of Arkansas, 1986.
- ⁹National Instruments Corporation, 11500 N. Mopac Expwy., Austin, TX 78759-3504.
- ¹⁰Idaho National Engineering and Environmental Laboratory, Idaho Falls, ID 83415.
- ¹¹H. Wollnik, in *Focusing of Charged Particles*, edited by A. Septier (Academic, Orlando, 1967), pp. 163–202.
- ¹²H. Wollnik, in *Optics of Charged Particles* (Academic, San Diego, 1987), p. 98.
- ¹³J. C. S. Kools, in *Pulsed Laser Deposition of Thin Films*, edited by D. B. Chrisey and G. K. Hubler (Wiley, New York, 1994), p. 457.